

Caliste 64: detection unit of a spectro imager array for a hard X-ray space telescope

A. Meuris^a, O. Limousin^a, F. Lugiez^b, O. Gevin^b, F. Pinsard^a, C. Blondel^a, I. Le Mer^a, E. Delagnes^b, M.C. Vassal^c, F. Soufflet^c, and R. Bocage^c

^aCEA, IRFU, Serv. Astrophys., F-91191 Gif-sur-Yvette Cedex, France

^bCEA, IRFU, Serv. Elec. Detect. Info., F-91191 Gif-sur-Yvette Cedex, France

^c3D Plus, 641 rue Hélène Boucher, F-78532 Buc, France

ABSTRACT

In the frame of the hard X-ray Simbol-X observatory, a joint CNES-ASI space mission to be flown in 2014, a prototype of miniature Cd(Zn)Te camera equipped with 64 pixels has been designed. The device, called Caliste 64, is a spectro-imager with high resolution event time-tagging capability. Caliste 64 integrates a Cd(Zn)Te semiconductor detector with segmented electrode and its front-end electronics made of 64 independent analog readout channels. This $1 \times 1 \times 2 \text{ cm}^3$ camera, able to detect photons in the range from 2 keV up to 250 keV, is an elementary detection unit juxtaposable on its four sides. Consequently, large detector array can be made assembling a mosaic of Caliste 64 units. Electronics readout module is achieved by stacking four IDeF-X V1.1 ASICs, perpendicular to the detection plane. We achieved good noise performances, with a mean Equivalent Noise Charge of ~ 65 electrons rms over the 64 channels. Time resolution is better than 70 ns rms for energy deposits greater than 50 keV, taking into account electronic noise and technological dispersal, which enables to reject background by anticoincidence with very low probability of error. For the first prototypes, we chose CdTe detectors equipped with Al-Ti-Au Schottky barrier contacts because of their very low dark current and excellent spectroscopic performances. So far, three Caliste 64 cameras have been realized and tested. When the crystal is cooled down to -10°C , the sum spectrum built with the 64 pixels of a Caliste 64 sample results in a spectral resolution of 664 eV FWHM at 13.94 keV and 841 eV FWHM at 59.54 keV.

Keywords: CdTe, Simbol-X, spectro-imager, X rays

1. SCIENTIFIC AND TECHNOLOGICAL CONTEXT

1.1 Simbol-X mission

The Simbol-X mission is a hard X-ray space telescope. It is currently undergoing a phase B with the French and the Italian space agencies. This telescope will fill the gap between X-ray telescopes with grazing mirrors, efficient until ~ 10 keV (XMM-Newton, Chandra missions) and hard X-ray and gamma-ray instruments using indirect imaging technique with coded masks to detect higher energies (INTEGRAL, SWIFT missions). Simbol-X will be a 20 meter focal length observatory, achieved by two satellites flying in formation. One carries the grazing incidence mirror to focus X-rays until 80 keV. The other satellite carries the detector payload. This focusing technique improves sensitivity and angular resolution by two orders of magnitude compared to the current instruments above 10 keV. As a consequence, a wide range of sources can be studied in detail, such as galactic and extra-galactic compact sources, supernovae remnants, cluster of galaxies, or young stellar objects. The core scientific objectives of Simbol-X are black holes physics and particle acceleration mechanisms [1,2].

The detection set consists of three detector units [3]. The Low Energy Detector is a silicon drift detector with DEPFET readout, also called "Macro Pixel Detector" [4]. It covers the energy range from 0.5 to 20 keV. The High Energy Detector (HED) installed below the first detector is efficient from 8 to 100 keV. The third unit is an active shielding to reject background (unfocused photons and protons) by temporal coincidence.

1.2 The High energy detector (HED)

The sensors for the HED are Cd(Zn)Te detectors with segmented electrodes. CdTe and CdZnTe are semiconductors well suited for X and gamma rays detection, with excellent properties for imaging and spectroscopy. Contrary to silicon, a 2 mm-thick CdTe detector is still 97% efficient at 80 keV. Contrary to germanium, it can be processed with small pixels size for imaging and it can be easily operated at room temperature or moderately cooled. Requirements for the instrument come from both imaging and spectroscopy constraints. A pixel pitch of 625 μm is necessary to properly sample the ~ 3 mm diameter HEW point spread function. The 12 arcmin field of view requires a detector array of 64 cm^2 . Detector material uniformity is also essential to guarantee high imaging quality. The spectroscopic performance baseline of 1.2 keV fwhm at 60 keV over all the channels of the HED is driven by the study of supernovae. To build explosive nucleosynthesis models in young supernovae, a key parameter is the abundance of the ^{44}Ti isotope, visible through the 68 and 78 keV lines emitted in its decay chain. High resolution spectroscopy is not possible without very low noise electronics. The HED specifications are summarized in the table below.

Table 1: High energy detector specifications

Parameter	Requirement
Energy band	8 – 80 keV
Efficiency	100 % at 30 keV > 90 % at 80 keV
Dimensions	8 \times 8 cm^2
Pixel size (pitch)	625 μm
Detector effective areas	> 90 %
Timing accuracy	
Science	50 μs
Anticoincidence	100 ns rms
Energy resolution	< 1.2 keV fwhm at 60 keV
Effective HED threshold	4 keV
Duration of observation	~ 10 ks

1.3 Caliste concept

Imaging requirements leads to a high energy detector with 16384 pixels. Each pixel has its own readout channel. One of the main technological difficulties is to integrate the front-end electronics. The solution contemplated is to put side by side 64 independent cameras of 256 pixels, with their front-end electronics below their 1 cm^2 detector. Caliste prototypes are designed to match Simbol-X scientific requirements while taking into account this strong constraint of integration.

Front-end electronics is achieved by full-custom IDeF-X ASICs. The solution to integrate the ASICs below the detector is to put the chips perpendicularly to the detection plane to read out two rows of pixels each. All the Caliste cameras are based on this principle of hybridization. The first prototype of the collaborative work between CEA/Irfu and 3D Plus company is Caliste 64, with four 16-channel ASICs to read out independently 64 pixels. The ASICs are mounted on mini printed circuits boards. The four PCBs are stacked and molded in an epoxy resin, according to 3D Plus technology [5]. The last step is the mounting of the detector on the top of the electronic block. The whole camera fits in a 1 \times 1 \times 2 cm^3 volume and is juxtaposable on its four sides. The whole fabrication respects space standards.

2. CALISTE 64 SUB-ASSEMBLIES

Caliste 64 is the hybridization of a 64-pixel Cd(Zn)Te detector with its front-end electronics. Detectors on one hand and ASICs on the other hand have been deeply studied before fabricating the camera.

2.1 Cd(Zn)Te detector

Crystals for Caliste 64 are Cd(Zn)Te matrixes of 8×8 pixels of $900 \mu\text{m}$ side. Gap between pixels is $100 \mu\text{m}$. The 64 pixels are surrounded by a $900 \mu\text{m}$ guard ring. Thickness is typically 1 or 2 mm.

CdTe and CdZnTe are very resistive semiconductors (10^9 to $10^{10} \Omega\cdot\text{cm}$ at room temperature). Their low dark currents enable to have low electronic noise and, as a consequence, potentially good spectroscopic performances. Samples from different families of detectors were mounted on substrates; current measurement in each pixel as well as spectroscopic measurement were realized at different temperatures with two dedicated test-benches [6]. Two kinds of detectors were identified as good spectrometers. 2 mm-thick CdZnTe detectors processed by Bruker Baltic (Latvia) from raw material produced by eV-products (USA) have current level of $\sim 1\text{pA}$ per pixel at -35°C when biased at -400V (Figure 1a). For one sample, excellent spectra were obtained with the 64 pixels (Figure 2a). CdTe detectors with Al-Ti-Au anode from Acrorad (Japan) show very good uniformity [7,8,9]. Due to the Schottky barrier contact, dark current is very low too [10]. The best spectroscopic results were obtained with 1 mm-thick samples biased at -400V (579eV fwhm at 13.94keV and 767eV fwhm at 59.54keV , -35°C). We chose to mount CdTe detectors on the first Caliste 64 cameras because we had obtained excellent results with the 6 samples of this family. Next batch of Caliste 64 will be equipped with CdZnTe detectors.

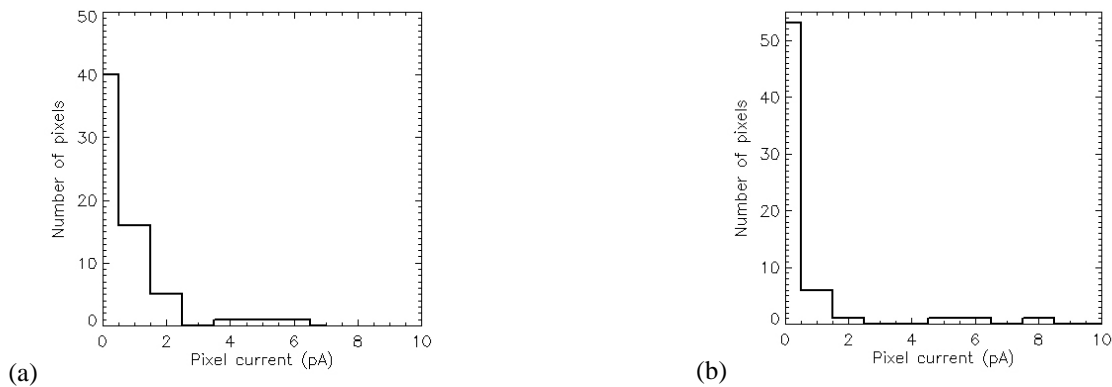


Figure 1: Histogram of pixel current of 64-pixel Cd(Zn)Te detectors at -35°C , -400V . (a) 2 mm-thick CdZnTe detector. (b) 2 mm-thick Schottky CdTe detector (63/64 pixels).

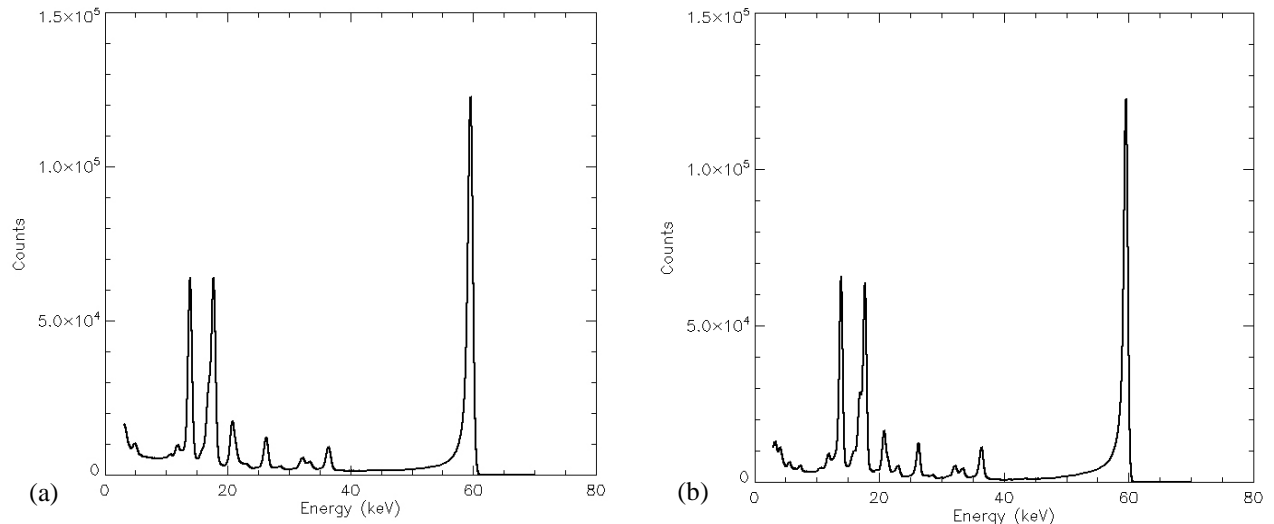


Figure 2: Sum spectra of 64-pixel Cd(Zn)Te detectors at -35°C . (a) 2 mm-thick CdZnTe detector, biased at -800V (64/64 pixels). Energy resolution is 0.72keV at 14keV and 0.93keV at 60keV . (b) 1 mm-thick Schottky CdTe detector, biased at -400V (63/64 pixels). Energy resolution is 0.58keV at 14keV and 0.77keV at 60keV .

2.2 Front-end electronics

The front-end electronics use full-custom ASICs named IDeF-X 1.1. Each analog channel includes a charge sensitive preamplifier (CSA) with a continuous reset system, a pole zero cancellation system (PZ) and a variable peaking time fourth order Sallen & Key type shaping filter (SK). After the filters, the signal is a pulse whose amplitude is proportional to the incident charge. A stretcher realized with a peak detector plus a storage capacitor stores the amplitude, whereas a discriminator raises a trigger signal when the output is above the low-level threshold. Each stretcher is connected to the output buffer through an analog multiplexer, so as the channel outputs be read one by one. Each discriminator output contributes to the trigger signal output through a 16 inputs logical OR circuit, so as a trigger signal be sent outside the circuit as soon as at least a channel reaches the threshold value. The low-level threshold is adjustable and common to all channels. A schematic view of the circuit is illustrated in Figure 3. Noise can be as low as 35 electrons rms with neither capacitance load nor detector current at the channel input. Power dissipation is 2.8 mW / channel. Moreover, the circuit is radiation hard up to 1 MRad, and so, it is compatible with space applications [11].

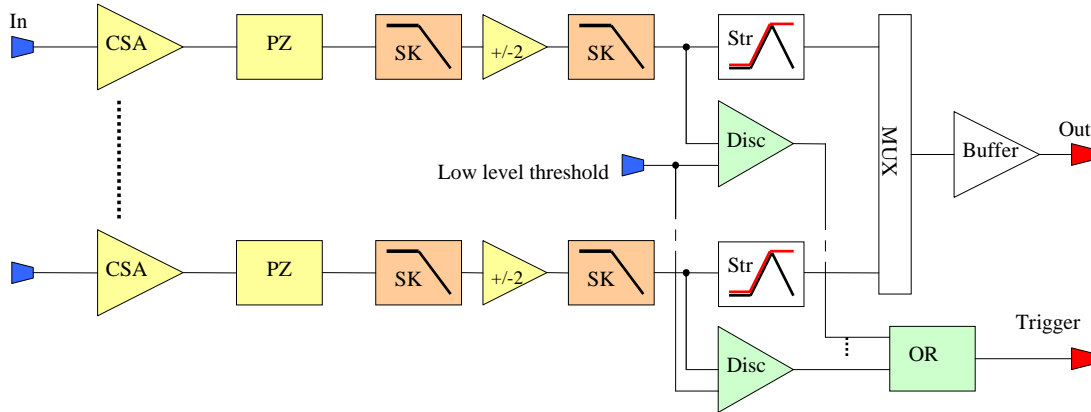


Figure 3: Schematic of the IDeF-X 1.1 circuit.

IDeF-X 1.1 is a 16-channel readout chip. As a consequence, 4 ASICs are integrated in the hybrid component to read out the 64 pixels individually. To connect each channel to a pixel, ASICs are first stacked in a $10 \times 10 \times 18 \text{ mm}^3$ block, perpendicularly to the detection surface. The top of this block is then prepared by laser ablation to get an 8×8 pixel pattern. The 16 pads of each ASIC are connected to 2 rows of 8 pixels.

3. ELECTRONIC PERFORMANCE

3.1 Set-up

Caliste 64 design was first validated without detector (see Figure 4). Charges generated by the interaction of a photon in the detector are simulated by a voltage step through a capacitance of 200 fF integrated in each channel. Since electronic performance depends on the dark current level of the detector, the device includes a tunable current source to produce leakage current at the input of each analog channel.

The acquisition is controlled by a printed circuit board with a FPGA. The readout sequence mode can be chosen (full-frame, hit pixels or hit pixels plus their neighbors), as well as the peaking time, the low-level thresholds, the frequency and the levels of the injections. The Caliste 64 sample, the FPGA and the computer communicate according a Spacewire protocol. For each event, the trigger time is recorded, as well as the pixel number and the amplitude of the differential output signal. That enables to perform imaging and spectroscopy with time tagging.

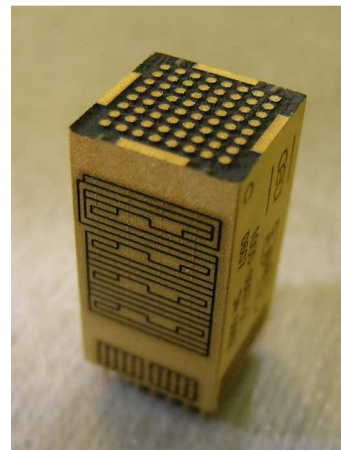


Figure 4: Electronic body of Caliste 64. Four ASICs are stacked inside a module and connected to the 8×8 pixel interface.

3.2 Electronic noise without detector

Noise performance is studied at different peaking times to know the minimum achievable noise and the associated optimal peaking time. For the shortest peaking times, the noise is dominated by the thermal noise of the preamplifier input MOSFET and increases linearly with the total capacitance connected at the channel input. The noise level for longer peaking times mainly depends on the dark current of the detector [12]. For a pixel current of about 7 pA, the minimum noise is ~65 e- rms for a peaking time value of 7.2 μ s (see Figure 5). This current level is typically what is expected with the Schottky CdTe detectors at -10°C.

The validation of electronics of a Caliste 64 sample consists in measuring gain and noise for different peaking times at room temperature to check that each of the 64 pixels have nominal performance. Figure 6 illustrates the homogeneity over 64 pixels.

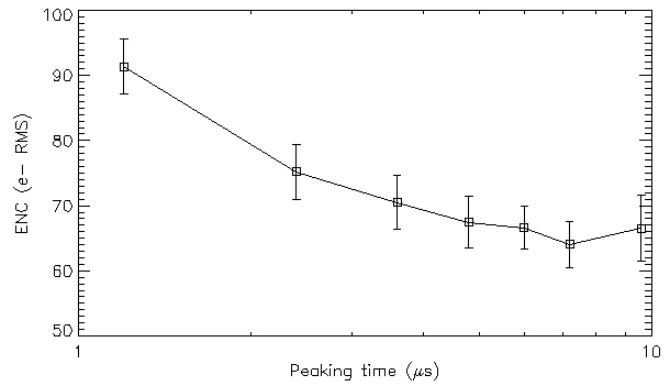


Figure 5: Mean equivalent noise charge of Caliste 64 electronics versus peaking time for a leakage current of ~7 pA. Error bars correspond to the standard deviation between the 64 channels.

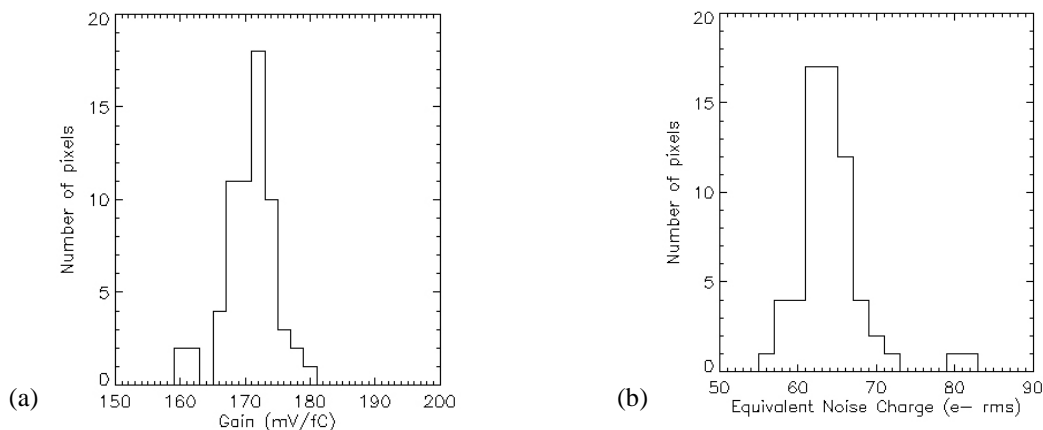


Figure 6: Electronic performance of a Caliste 64 sample, at 7.2 μ s peaking time, for a leakage current of about 7 pA. (a) Histogram of the gain of the 64 pixels. (b) Histogram of the equivalent noise charge of the 64 pixels.

3.3 Timing

Caliste 64 is a spectro-imager with time-tagging capability. To find precisely the time of arrival of a particle from the trigger time, one must correct the timewalk of the signal, taking into account the low-level threshold, the peaking time value and the collected energy (see Figure 7). After this compensation, some errors, assumed independent, remain:

- The technological mismatch is responsible for a difference of transfer functions between the channels, and as a result, a difference on trigger times. This error is noted Δt_{mis} .
- Noise on the signal (and on the threshold level) is responsible for variations on the timewalk for a single channel. This error is noted Δt_N .
- The difference of interaction depth in the Cd(Zn)Te semiconductor detector induces different transit times (because holes are much slower than electrons), responsible for variations on trigger delay.

With the Caliste 64 electronic body, we can estimate the first two sources of errors. We inject given amplitude a high number of times and we register for each pixel the delay between the injections and the triggers. We obtain for each pixel a random variable TW_i , modeled as a Gaussian with moments μ_i and σ_i . The timewalk correction to apply to the Caliste 64 sample is the mean of the μ_i distribution (see Figure 7b). Δt_{mis} is the standard deviation of the μ_i distribution (see Figure 8a). The typically Δt_N error of a channel is the mean of the σ_i distribution (see Figure 8b). We can repeat the experiment for several levels of injections and several peaking times. For 50 keV particles, error due to mismatch is 33 ns rms and error due to electronic noise is 59 ns rms, for the higher peaking time value. That means that time resolution is better than 70 ns rms for energies greater than 50 keV, taking into account only the front-end electronics contribution. In Simbol-X focal plane, the constraint on time resolution concerns high energy particles for anticoincidence processing. Front-end electronics induces an error on time-tagging inferior to 50 ns rms for energy deposits greater than 150 keV.

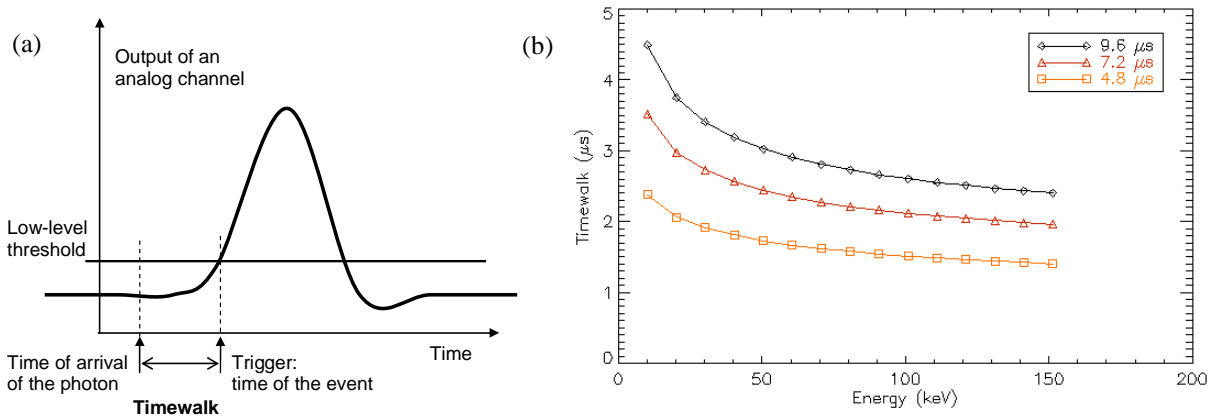


Figure 7: Timewalk calibration. (a) Definition of timewalk. (b) Mean timewalk over 64 pixels, for a 3 keV low-threshold.

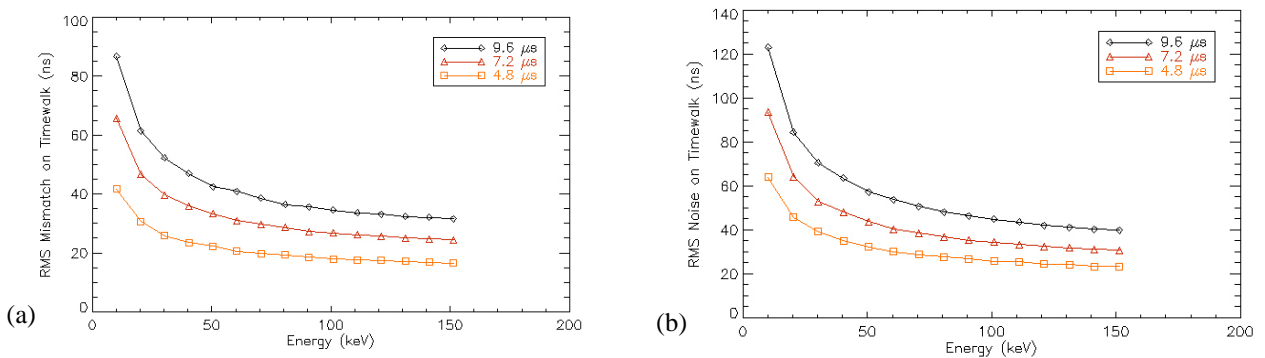


Figure 8: Estimation of time-tagging errors due to electronics, with respect to the deposited energy, for a 3 keV threshold. (a) Δt_{mis} error due to technological mismatch between the 64 pixels of the device. (b) Mean Δt_N error due to electronic noise on each pixel.

4. SPECTROSCOPY

4.1 Operations

After the electronic part of the Caliste 64 camera has been tested and validated, a 64-pixel detector is mounted on the top of the device. A 100 μm gold wire is installed on the planar cathode to provide the high voltage supply (see Figure 9). The camera is placed in a thermal enclosure with a ^{241}Am source to perform spectroscopic tests at different temperatures. The set-up is exactly the same as the one for electronic characterization. Until now, the minimum achievable temperature is -15°C at the detector level.

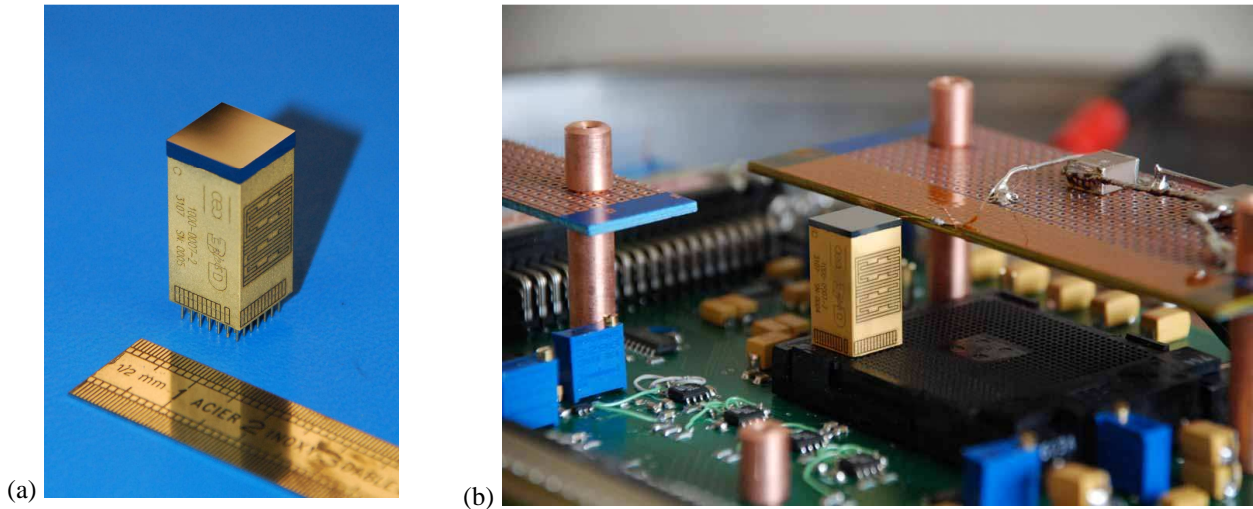


Figure 9: Caliste 64 complete camera. (a) The sample with 2mm-thick Schottky CdTe detector fits in a $1 \times 1 \times 2 \text{ cm}^3$ volume. (b) Integration in the thermal enclosure of a Caliste 64 sample, connected to the high voltage by a $100 \mu\text{m}$ gold wire.

Three complete cameras were tested, with 1 and 2 mm-thick CdTe Schottky detectors from Acrorad. All of them have 64 pixels with good spectroscopic quality.

4.2 Individual performance and Sum spectrum

For a Caliste 64 sample, each pixel is precisely calibrated to obtain spectra with one channel per 10 eV. Individual spectral resolutions are computed. Figure 10 shows that the 64 pixels have very homogenous spectral performances (energy resolution of $\sim 0.7 \text{ keV}$ at 14 keV and 0.85 keV at 60 keV, when the detector is cooled down to -15°C). Then sum spectra are obtained by summing the 64 individual calibrated spectra channel by channel (see Figure 11 and Table 2). Sometimes, one or two pixels are excluded from the sum because they have a bit too much current and their spectra are out of global statistics. By cooling down to -30°C , we should improve uniformity and include all the pixels in the sum.

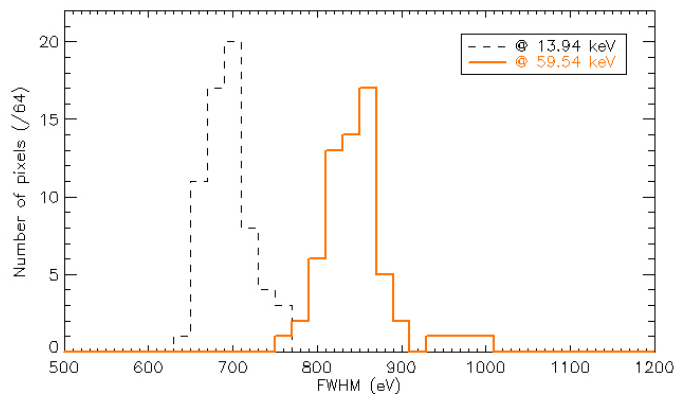


Figure 10: Spectral resolution of the 64 pixels of a Caliste 64 camera, with a 1 mm thick detector cooled down to -15°C and biased at -400°C . Mean energy resolution is 705 eV FWHM at 13.94 keV and 858 eV FWHM at 59.54 keV.

Table 2: Characteristics of the sum spectra illustrated in Figure 11. The number of pixels included in the sums are respectively 63, 64 and 62 in SN3, SN4 and SN5. Detector temperature is about -10°C . Energy resolutions correspond to FWHM. Peak to valley ratio is computed as the ratio of the counts at 59.54 keV by the counts at 57 keV.

Sample	Thickness	Bias voltage	Peaking time	ΔE @14 keV	ΔE @60 keV	Peak to valley ratio (59.54 / 57 keV)
SN3	1 mm	400 V	6 μs	694 eV	851 eV	44
SN4	1 mm	500 V	9.6 μs	664 eV	841 eV	55
SN5	2 mm	800 V	4.8 μs	735 eV	905 eV	34

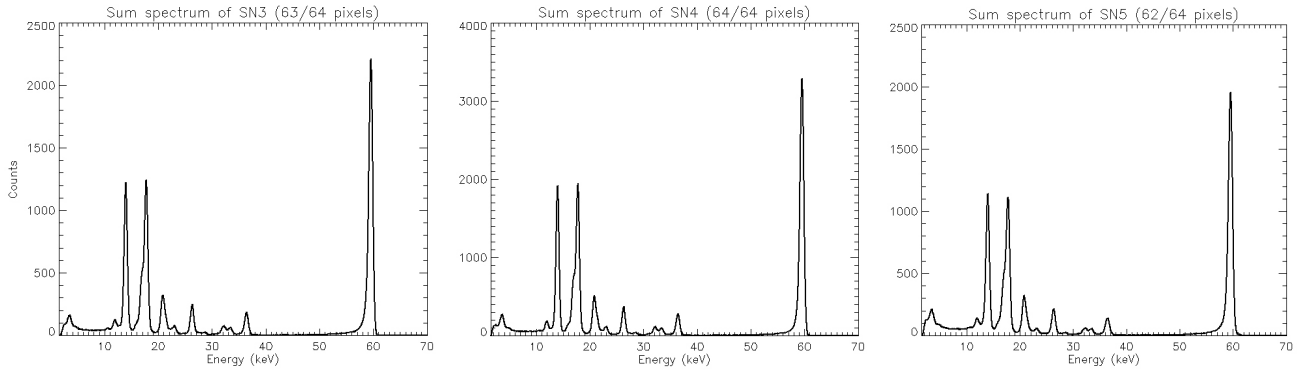


Figure 11: Best sum spectra obtained with the three first Caliste 64 samples, for CdTe detectors cooled down to -10°C . SN3 and SN4 (left and center) are equipped with 1 mm thick detectors. SN5 on the right is equipped with a 2 mm-thick detector.

4.3 Split events

Caliste 64 enables to perform spectroscopy with time resolution. As a consequence, split events can be easily studied by selecting events in coincidence between neighbor pixels. Split events occur in case of charge sharing when a photon interacts in-between pixels and induces signals on several electrodes, or when the first interaction in a pixel with a Cd or a Te atom produces an X-ray fluorescence photon that escapes in the neighbor pixel. Figure 12 shows the correlation between the energies of any couple of pixels that triggered at the same time. For a 1 mm-thick detector biased at -400V , that double events correspond to $\sim 10\%$ of the events. The sum of the energies gives singular constants corresponding to the Americium lines. The straight lines indicate that there is very little charge, even when the photon interacts in the pixel gap.

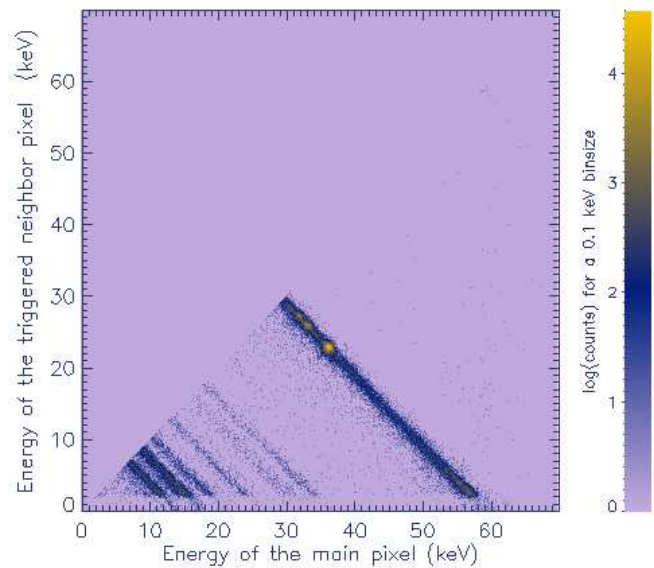


Figure 12: Correlation graph of the energies of any couple of pixels that trigger at the same time. The energy is calibrated for each pixel from its single events spectrum.

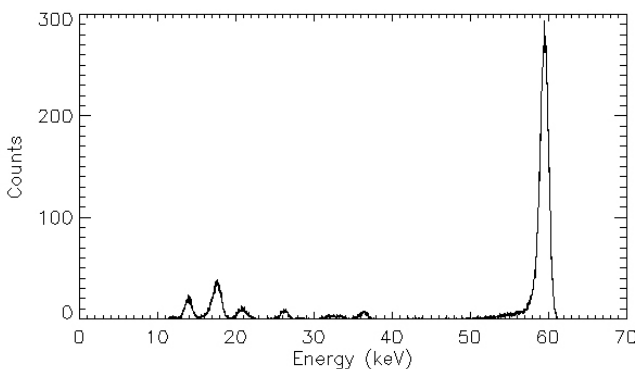


Figure 13: Spectrum built with only the split events between two pixels, at -10°C . Energy resolution is 1.23 keV at 60 keV.

The spectrum reconstructed from double events is shown in Figure 13. After summing the energies of the couple pixels, the main line is centered on 59.23 keV instead of 59.54 keV. As result, we estimate charge loss, at this energy, as:

$$CL = \frac{59.54 - 59.23}{59.54} = 0.52\%$$

An extra calibration is performed to compensate this little charge loss. We obtain an energy resolution is 1.23 keV at 60 keV at -10°C. When comparing this resolution ΔE^{double} with the spectral resolution ΔE^{single} with only single events, we notice that:

$$\Delta E^{double} \approx \sqrt{2} \Delta E^{single}$$

This is consistent with the best achievable resolution after summing noise of two independent detection channels. Moreover, even the resolutions obtained at -10°C for the double events are very close to the Simbol-X requirements, so that the latter will certainly be met for the expected -35°C operation temperature

5. CONCLUSION

Caliste 64 is the new spectro-imager designed for space applications, in particular for large hard X-ray focal planes. Its high performance meets Simbol-X requirements in terms of spectroscopy and time-tagging accuracy. Spectral resolution is already excellent at -10°C (~0.85 keV fwhm at 59.54 keV). Cooling down the detector to -35°C will guarantee uniformity and energy resolution better than 1.2 keV fwhm at 60 keV over all the channels. Contribution of front-end electronics on time-tagging error is inferior to 50 ns rms for energies greater than 150 keV. Taking into account the influence of CdTe detector itself and even errors of timewalk quantification in the embedded calibration tables, the device is likely to fulfil time resolution requirement of 100 ns rms. As a result, background can be rejected from HED data by temporal anticoincidence with a very low probability of error. Next challenge is a new prototype with 256 pixels in the same volume as Caliste 64 to reach the spatial resolution of 625 μm needed for Simbol-X mission. The fabrication of this micro-camera called Caliste 256 is being studied by CEA/Irfu and 3D Plus.

ACKNOWLEDGEMENTS

The authors would like to thank the CNES (French National Space Agency) for their support to this work.

REFERENCES

- [1] Ferrando P., Arnaud M., Briel U. et al., "Simbol-X: mission overview", *Proc. SPIE conf.* **6266** (2006).
- [2] Pareschi G., Ferrando P., "The Simbol-X hard X-ray mission", *Exp. Astron.* **20**, 139-149 (2005).
- [3] B.P.F. Dirks et al., "The focal plane of the Simbol-X space mission", *Proc. SPIE conf.* **6276** (2006).
- [4] J. Treis et al., "DEPFET Based Focal Plane Instrumentation for X-Ray Imaging Spectroscopy in Space", *Proc. IEEE NSS-MIC conf. rec.*, 2226-2235 (2007).
- [5] C. Val, M. Leroy, Patent 90 15473, 3D Plus, dec. 1990.
- [6] A. Meuris et al., "Caliste 64, an innovative CdTe hard X-ray micro-camera", *IEEE Trans. Nucl. Sci.* **55** (2), 778-784 (2008).
- [7] H. Toyama et al., "Formation of aluminium Schottky contact on plasma-treated cadmium telluride surface", *Jpn. J. Appl. Phys.* **43**, 6371-6375 (2004).
- [8] H. Toyama et al., "Effect of He plasma treatment on the rectification properties of Al/CdTe Schottky contacts", *Jpn. J. Appl. Phys.* **44**, 6742-6746 (2005).
- [9] S. Watanabe et al., "New CdTe Pixel Gamma-Ray Detector with Pixelated Al Schottky Anodes", *Jpn. J. Appl. Phys.* **46**, 6043-6043 (2007).
- [10] T. Takahashi and S. Watanabe, "Recent Progress in CdTe and CdZnTe detectors", *IEEE Trans. Nucl. Sci.* **48** (4), 950-959, (2001).
- [11] F. Lugiez, et al., "IDeF-X V1.1: Performances of a New CMOS 16 Channels Analogue Readout ASIC for Cd(Zn)Te detectors", *Proc. IEEE NSS-MIC conf. rec.*, 841-844 (2006).
- [12] V. Radeka, P. O'Connor, "Integrated Circuits Front Ends for Nuclear Pulse Processing", IEEE NSS Short Course, Toronto (1998).